Nanoscale

Study of Cytochrome c–DNA Interaction - Evaluation of Binding Sites on the Redox Protein

Journal:	*Nanoscale*
Manuscript ID:	NR-ART-09-2014-005301
Article Type:	Paper
Date Submitted by the Author:	11-Sep-2014

Complete List of Authors:	Wettstein, Christoph; Technical University of Applied Sciences Wildau , Biosystems Technology Kyne, Ciara; NUI Galway, Chemistry Doolan, Aishling; NUI Galway, Chemistry Mohwald, Helmuth; Max-Planck Inst. of Colloids and Interfaces, Department of Interfaces Crowley, Peter; NUI Galway, Chemistry Lisdat, Fred; Technische Hochschule Wildau, Biosystems Technology

Study of Cytochrome *c*–DNA Interaction - Evaluation of Binding Sites on the Redox Protein

Christoph Wettstein,[ac] Ciara Kyne,[b] Aishling Doolan,[b] Helmuth Möhwald,[c] Peter B. Crowley[b*] and Fred Lisdat.[a*]

[a] *Technical University of Applied Sciences Wildau, Institute of Applied Life Sciences, Biosystems Technology, Hochschulring 1, 15745 Wildau, Germany*

[b] *National University of Ireland Galway, School of Chemistry, University Road, Galway, Ireland*

[c] *Max-Planck Institute of Colloids and Interfaces, Department of Interfaces, Am Mühlenberg 1, 14424 Potsdam, Germany*

Corresponding Authors

* Peter B. Crowley: Phone: +353 (0) 91 49 24 80; email: peter.crowley@nuigalway.ie

* Fred Lisdat: Phone: +49 (0) 3375 / 508 456; email: flisdat@th-wildau.de

KEYWORDS. protein-nucleic acid interactions, multilayer assemblies, NMR spectroscopy, transient complexes

ABSTRACT.

Artificial assemblies consisting of the cationic cytochrome *c* (cyt *c*) and double-stranded DNA are interesting for the field of biohybrid systems because of the high electro-activity of the incorporated redox protein. However, little is known about the interactions between these two biomolecules. Here, the complex of cyt *c* and a 41 base pair oligonucleotide was characterized in solution as a function of pH and ionic strength. Persistent cyt *c*-DNA agglomerates were observed by UV-vis and DLS (dynamic light scattering) at pH 5.0 and low ionic strength. The strength of the interaction was attenuated by raising the pH or the ionic strength. At pH 7.0 agglomerates were not formed, allowing interaction analysis by NMR spectroscopy. Using TROSY (transverse relaxation-optimized spectroscopy)-HSQC (heteronuclear single quantum coherence) experiments it was possible to identify the DNA binding site on the cyt *c* surface. Numerous residues surrounding the exposed heme edge of cyt *c* were involved in transient binding to DNA under these conditions. This result was supported by SEC (size exclusion chromatography) experiments at pH 7.0 showing that the interaction is sufficient for co-elution of cyt *c* and DNA.

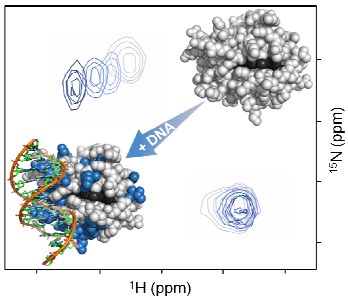

The characteristics of cyt *c*-DNA complexation change from transient to permanent in dependency on the pH value and the ionic strength. Hereby, typical binding sites known from cyt *c*-protein complex formation are affected by DNA.

INTRODUCTION.

Protein-DNA interactions are of fundamental importance to the living cell and involve nonspecific and specific processes.[1] Specific binding takes place when residues interact with a particular DNA sequence and can be found *e.g.* with enzymes[2,3] and transcription factors.[4,5] This kind of interaction can be accompanied by intercalation of residues between the base pairs (after unwinding of the DNA) or protein binding to DNA secondary structures such as loops or G-quadruplexes.[6-8] Nonspecific binding, which often precedes specific binding, arises from charge-charge interaction between cationic residues and the anionic phosphate backbone.[1,9] This association is often weak under medium ionic strength conditions. Stronger binding occurs by the insertion of an α-helix into the major groove of the DNA.[10] Since these complexes lack hydrophobic interactions they were found to be significantly less stable than the specific ones.[11]

Addressing biotechnological approaches, artificial protein-ligand complexes have been investigated recently. For instance, the interaction of cyt *c* and the small protein recognition molecule, calixarene which disguises the protein surface and alters its interaction behaviour, was studied.[12] Alternatively 3D DNA designs (also known as DNA origami),[13] capable of holding proteins while preserving their function, were described.[14-16] In the field of bioelectronics especially surface confined protein arrangements are relevant. One strategy is dedicated to the formation of fully electro-active protein architectures on electrodes. For this purpose, the redox protein cytochrome *c* (cyt *c*) and double stranded DNA were utilized as building blocks.[17]

Cyt *c* is a small, α-helical, redox protein that functions as an electron shuttle in mitochondrial respiration.[18] Horse heart cyt *c* has been extensively studied as a model protein for heterogeneous electron transfer (ET)[19,20] and has been used as a recognition element in biosensors.[21-25] Horse heart cyt *c* has a basic p*I* of 10.0-10.5 and the abundant lysine residues encircling the heme

edge[26] contribute to fast inter-protein ET by electrostatic steering.[27,28] The positively charged surface patches also cause the 'stickiness' of the protein which results in strong, unspecific interactions.[29] Moreover, charge-charge interactions of lysines with negatively charged functionalities on surfaces can occur *e.g.* with SAMs. This provides the basis for an efficient and oriented immobilisation on electrodes.[30,31]

Protein-DNA interactions have also been used in the field of bioelectrochemistry. In the 1990s ET between cyt *c* and electrodes was studied in the presence of DNA under different conditions.[32] Charge-charge interactions have been exploited to immobilize cyt *c* on DNA modified electrodes and promote direct electrochemistry of cyt *c*.[33-35] DNA has also been used as a building block for the assembly of cyt *c* into multilayers[17,36] Cyt *c*-DNA multilayer systems were created by the layer-by-layer deposition technique on modified gold electrodes. Such assemblies were found to be formed only at pH 5.0 but not under neutral conditions. Cyclic voltammetry of multilayer assemblies showed quasi-reversible ET, a substantial amount of electro-active protein (up to 320 pmol/cm^2 for a 6 bi-layer system) and only minor changes in the formal redox potential (E_f) of cyt *c*, indicating that the heme remains in the native state.[17] Compared to other multilayer systems (built using synthetic polyelectrolytes or modified nanoparticles[37-39]) the cyt *c*-DNA system showed the highest accumulation of redox active material. Exploiting these properties, cyt *c*-DNA multilayer systems were advanced to construct analytical signal chains. For example, a glucose sensitive electrode was constructed by combining a cyt *c*-DNA multilayer with pyrroloquinoline quinone dependent glucose dehydrogenase (PQQ-GDH).[36] Similarly, the enzyme cellobiose dehydrogenase (CDH) could be incorporated into the cyt *c*-DNA architecture to afford the system a sensitivity towards lactose, the enzyme´s substrate.[40]

These developments illustrate the application potential for cyt *c*-DNA interactions but they are not limited to bio-electrochemistry, since actual developments in creating 3D-structures made from nucleic acids can also pave the way for a defined positioning of proteins in bio-hybrid systems.[14-16] Although the electrostatic nature of the cyt *c*-DNA interaction was already studied, little is known about the structural details and the pH dependence. Therefore, we now focus on the binding conditions and the elucidation of possible interaction sites of the redox protein with double stranded DNA molecules.

RESULTS AND DISCUSSION

Previous work with cyt *c*-DNA multilayer systems used calf thymus (ct) DNA as a building block.[17] Agarose gel electrophoresis of ct DNA revealed that it was a mixture of fragments of varying size (Figure S1). Here, in order to work with a better defined system, we used a double stranded DNA comprising 41 bp oligonucleotides.

Cyt *c*-DNA Interactions and Agglomeration. The interactions between cyt *c* and DNA were characterized at different pH and salt conditions in order to get more insights into the nature of the biomolecular interaction. Samples of cyt *c* and DNA at pH 5.0 and low ionic strength (10 mM NaCl) were observed to turn cloudy in approximately 10 seconds. After mixing, the UV-vis spectrum had an increased absorbance over the whole wavelength range indicating the formation of agglomerates, which cause light scattering (Figure 1a). These agglomerates had an average diameter of 1250 ± 200 nm as determined by DLS (Figure S2). Acquiring the spectrum of the cyt *c*-DNA mixture over a period of hours showed a decrease in absorbance, indicating the precipitation of the agglomerates. Increasing the salt concentration recovered the characteristic

cyt *c* spectrum, with partial disruption of the agglomerates at 50 mM NaCl and an almost complete recovery of the cyt *c* spectrum at 100 mM NaCl (Figure 1a). DLS measurements on the latter sample revealed the presence of particles with a size of 400 ± 200 nm despite the high salt concentration. This indicated that the cyt *c* and DNA interact even at high ionic strength. The precipitation at pH 5.0 and low ionic strength correlated well with the previous findings of efficient deposition of cyt *c* on DNA (and vice versa) that resulted in stable multilayer assemblies.[32] We conclude that the interaction between the two biomolecules does not only proceed on a surface; it is strong enough to result in precipitation in solution.

Figure 1

At pH 7.0, mixtures of cyt *c* and DNA yielded UV-vis spectra identical to the pure protein, even after an incubation time of 60 min (Figure 1b). DLS measurements confirmed the absence of detectable particles. This suggested that the formation of larger agglomerates was suppressed at neutral pH, because of the modified charge density on the surface of both biomolecules. The pH stability of the cyt *c*-DNA complexes was investigated by taking a sample prepared at pH 5.0 and raising the pH to 7.0. The precipitated complexes remained insoluble. This is consistent with previous studies of cyt *c*-DNA architectures, which were assembled at pH 5.0 and remained stable when transferred to pH 7.0 measuring buffer.[17]

Secondary structure of cyt *c* in the presence of DNA. The secondary structure of cyt *c* in the presence of DNA was analyzed as a function of pH and ionic strength. Cyt *c* is rich in α-helical structures and has a characteristic CD spectrum with minima at 222 nm and 208 nm and an intense maximum at 192 nm (Figure 2).[46-48] Measurements were performed at pH 5.0 and 100 mM NaCl to avoid the formation of large agglomerates. Since Cl^- disturbs the CD signal in the

far UV region only the α-helical double minimum was considered here. The addition of DNA had no effect on the spectrum (Figure 2a), indicating no alteration of the α-helical structure under these conditions. The same was valid for pH 7.0 and low ionic strength (Figure 2b). It was also tested, whether CD spectra could be obtained at pH 5.0 and low ionic strength (10 mM NaCl). Although agglomeration occurred, reproducible spectra were obtained and small changes in the peak intensities were observed. However, the interpretation of this data is difficult owing to the process of precipitation.

Figure 2

The DNA binding site on cyt *c* revealed by NMR. Since precipitation of cyt *c*-DNA complexes precludes the acquisition of reliable NMR spectra, sample conditions were selected that minimized this process. Thus, interaction was first characterized at pH 7.0 with 30 mM NaCl. Figure 3 shows regions of the cyt *c* spectrum in the presence of increasing amounts of DNA (DNA:cyt *c* ratio from 0.06 to 0.48). Significant line broadening was observed upon the addition of DNA and reliable data could be obtained only with the TROSY-HSQC pulse sequence, which improves the resolution of the NMR spectra of molecules or complexes with high molecular weights. Concentration-dependent chemical shift perturbations (Δδ) were observed for numerous resonances while some resonances were broadened beyond detection. Saturation of these effects was observed at a DNA concentration of 18 μM (DNA:cyt *c* ratio 0.36) (Figure 3). These spectral changes were generally consistent with a fast exchange process on the NMR time scale and suggest that cyt *c* and the oligonucleotide formed a transient complex with a lifetime of milliseconds.[12,43,49,50]

Figure 3

Mapping the chemical shift perturbations (Δδ) to the crystal structure of cyt *c* revealed a broad patch, mainly involving residues in the N- and C-termini. This patch surrounds the exposed heme edge and corresponds to the known binding site of cyt *c*[12,28,51] (Figure 4). Several lysines (K7, K8, K72, K73, K86, K87 and K100) are involved in this site, suggesting that they may contribute to binding the anionic phosphate backbone of the DNA. Moreover, neutral residues in the close environment of the affected lysine residues also tend to show Δδ. The Q16 side chain, located right in front of the heme and a pivotal group in complex formation with protein partners[43,52] was also affected by DNA binding. Therefore, it appears that the anionic, rod-like DNA can mimic the general features of natural binding partners.

Figure 4

NMR data was also collected at pH 6.0 (Figure S3). The observed changes in the NMR were similar to those at pH 7.0; however, more residues were affected at the same DNA concentrations. This is consistent with an increased interaction under acidic conditions. Additional Δδ were observed even at lower DNA concentration, including the basic residues K5 and K88 as well as the neutral N70, Y74, E92 and A101. Moreover, Q12, C17, G37 were affected. The significant Δδ were summarised in Table 1 for a better comparison with the data obtained at pH 7.0. The increased number of residues affected at pH 6.0 suggests that at pH 5.0 even more sites may be involved, thus contributing to the strong interaction, which enables the formation of cyt *c*-DNA aggregates in solution and stable cyt *c*-DNA architectures on surfaces.[17]

Table 1

HSQC experiments were also performed at pH 5.0 with 100 mM NaCl. Under these conditions the interaction was not detected_by UV-vis but resulted in complexes which were stable in solution. The cyt *c*-DNA samples showed Δδ especially at the lysine residues K5, K8,

K88 and K89. This supports the idea that cyt *c*-DNA interaction is not completely inhibited even at a high ionic strength and may explain the small agglomerates found in DLS. When performed at a lower ionic strength of 50 mM NaCl, agglomeration was not completely suppressed. Thus, spectra of lower intensity and quality were acquired which were unsuited to further analysis.

SEC Analysis of cyt *c*-DNA interactions. We found at pH 5.0, cyt *c* and the oligonucleotide interacted persistently in the formation of agglomerates (as evidenced by UV-vis and DLS). At pH 7.0 the interactions were weaker and agglomeration did not occur. Here, the NMR studies revealed transient complex formation. Size exclusion chromatography (SEC) was performed to test whether the interaction was strong enough to have practical implications. SEC analysis was carried out on mixtures containing similar concentrations of cyt *c* and DNA, and identical buffer conditions as the NMR experiments (Figure 5). Pure cyt *c* (~13 kDa) eluted from the SEC column at a volume of 80-90 mL.[29] The mixtures of cyt *c* and DNA gave rise to a peak corresponding to the pure protein as well as a peak at 50-55 mL, which suggests a molecular weight of ~70 kDa (The 66 kDa BSA elutes from the column at 55 mL, but the rod-shaped DNA will elute differently to globular proteins). The 41 bp DNA alone has a molecular weight of ~25 kDa. The small peak at ~48 mL corresponds to the void volume of the column and indicates complexes or aggregates >150 kDa. SDS-PAGE analysis confirmed the presence of cyt *c* in the 50-55 mL fraction (Figure 5). In addition, the co-elution of the DNA-cyt *c* complex indicates that the K_d is in the μM range or lower. Interestingly, the suggested molecular weight of 70 kDa is consistent with the need to use TROSY-HSQC to obtain NMR data.

Figure 5

CONCLUSION.

The motivation for the present study was to gain some insight into cyt *c*-DNA interactions, which form the basis of multilayer assemblies on electrodes. For the assembly process on electrodes the best deposition was found at pH 5.0 and low ionic strength. The study with both bio-molecules in solution showed fast agglomeration indicating a strong interaction between cyt *c* and DNA at pH 5.0. The agglomeration proceeded within seconds and subsequent sedimentation occurred over hours. The interaction between the two biomolecules was drastically diminished by increasing the salt concentration to 100 mM NaCl but could not be completely suppressed. At higher pH values the interactions were much weaker. This suggests that two types of pH-dependent cyt *c*-DNA interaction occur: The NMR and SEC data confirm that transient interactions occurred at pH 7.0, which fits well to the cyt *c* function as an electron shuttle, capable of weak interactions with membranes and reaction partners. Importantly, NMR analysis revealed that the known binding sites of cyt *c* serve as interaction sites for DNA. However, under acidic conditions, the interaction with DNA was enforced, resulting in permanent complex formation and subsequent precipitation. This provides the basis for the technical application of cyt *c*-DNA multilayer assemblies. To gain a precise understanding of the interaction at pH 5.0, solid state NMR or X-ray crystallography would be required.

EXPERIMENTAL METHODS

Materials. Horse heart cytochrome *c* (cyt *c*), ascorbic acid, D_2O and spermine were purchased from Sigma Aldrich (Taufkirchen, Germany). SDS was purchased from Riedel-de Haën (Seelze, Germany). KH_2PO_4 (KPi) was provided by Merck and NaCl by Fluka. Complementary oligonucleotide strands with the sequence:

5'-CCCTCATAGTTAGCGTAACGGCAAATGGCATTCTGACATCC-3'

were synthesised by Biomers (Ulm, Germany) and Eurofins (Ebersberg, Germany). The protein and the DNA were dissolved in buffer and used without further purification. All solutions were prepared in deionised, 18 MΩ Millipore-water (Eschborn, Germany). Although different concentrations of protein and DNA were necessary, the same range of DNA:cyt *c* concentration ratios, *i.e.* 0.06 – 0.48, were used throughout this study.

^{15}N-labelled cyt *c* production and purification. ^{15}N-labelled horse heart cyt *c* was expressed in *Escherichia coli* BL21 (DE3)[41] and purified according to literature methods.[42,43] The purity and concentration of the protein was estimated by using 15 % SDS polyacrylamide gel electrophoresis (SDS-PAGE) and UV-vis spectroscopy (Perkin Elmer Lambda 35) with an extinction coefficient of $\varepsilon_{550} = 29.5\ mM^{-1}\ cm^{-1}$ for the reduced (ferrous) species.[44] Ferrous cyt *c* was prepared by the addition of 1 mM sodium ascorbate. ^{15}N-labelled cyt *c* was oxidised with an excess of $K_3[Fe(CN)_6]$ and exchanged into NMR buffer (20 mM KPi, 30 mM NaCl, pH 6.0) prior to concentration and storage at -20° C.

DNA hybridization. The oligonucleotide comprised 41 base pairs (bp), had a GC content of 50 % and a melting point (T_m) of 75° C. HPLC-purified single stranded DNA was provided as a lyophilized powder, containing sodium counter ions. Residues of triethylammonium acetate were also present. Single-stranded DNA was dissolved to 100 pmol/µl and shaken at 900 rpm for 15 minutes at room temperature (RT). The complementary strands were mixed in equimolar ratio,

heated to 68° C whilst shaking for 15 min and subsequently cooled to RT. Hybridization was confirmed by agarose gel electrophoresis (Figure S1).

UV-vis spectroscopy. A Thermo Scientific Evolution 300 spectrometer (Weltham, MA, USA) equipped with Peltier temperature control was used to collect spectra (350-600 nm) at 20° C. Agglomeration data were collected with 5 min intervals, while 2 min intervals were used when disrupting the complexes. Solutions of 18 μM reduced cyt *c* in 20 mM KPi plus 10, 50 or 100 mM NaCl and 0.1 mM ascorbic acid were incubated for 10 min at RT. The pH was adjusted and 3 μM oligonucleotide was added (DNA:cyt *c* ratio 0.17). The sample was mixed by gently inverting ten times and the pH was controlled.

Dynamic Light Scattering. A Beckman Coulter Delsa Nano c Particle Analyzer (Krefeld, Germany) was used to collect DLS data at a fixed scattering angle of 165°. The particle size distribution was calculated by using the Marquardt algorithm. The hydrodynamic diameter of the agglomerates was monitored by acquiring 200 data points in three cycles for each sample. The samples from the UV-vis experiments were used for DLS analysis.

Circular dichroism spectroscopy. CD measurements were carried out using a JASCO J-720 spectrometer (Tokyo, Japan) at RT using a quartz cuvette with 0.1 cm path length. Spectra were recorded on samples identical to those used for the UV-vis experiments, with a scan speed of 50 nm/min and 0.2 nm resolution. Each spectrum was calculated as an average of 6 scans. The samples were prepared in concentrations of 10 μM cyt *c* and 1.2 μM DNA (DNA:cyt *c* ratio 0.12) and incubated as for the UV-vis experiments.

NMR spectroscopy. All of the NMR samples contained 50 μM ^{15}N cyt *c*, 20 mM KPi, 30 mM NaCl and 10 % D_2O. After each DNA addition of 3, 6, 18 or 24 μM (DNA:cyt *c* ratios 0.06, 0.12, 0.36 and 0.48), the sample was gently inverted ten times and left to equilibrate at RT for 60

min. The pH was adjusted to the correct value prior to each measurement. 2D ^{1}H-^{15}N TROSY-(transverse relaxation-optimized spectroscopy) HSQC (heteronuclear single quantum coherence) spectra were acquired at 303 K with 32 scans and 64 increments, on a Varian 600 MHz NMR spectrometer equipped with a HCN cold probe and processed using linear prediction. The analysis of the DNA-induced chemical shift perturbations was performed in CARA (www.nmr.ch). The resonance assignments of reduced cyt *c* were based on those reported previously.[45]

Size exclusion chromatography. An Äkta FPLC equipped with an XK 16/70 column (1.6 cm diameter, 65 cm bed height) packed with Superdex 75 (GE Healthcare)[29] and operating at 21° C was used for SEC analysis of samples containing 100 μM cyt *c* and 9, 18 or 36 μM DNA (DNA:cyt *c* ratios 0.09, 0.18 and 0.36). A continuous flow rate of 1.5 mL/min was employed and the elution buffer was 20 mM KPi, 30 mM NaCl, pH 7.0. The protein content was followed at 280 nm and the SEC fractions were analysed in 15 % polyacrylamide gels.

ACKNOWLEDGEMENTS

The authors would like to thank Dr. Juan Giner-Casares and Prof. Dr. Gerald Brezesinski for their contribution to this project. Financial support was provided by the International Max-Planck Research School (IMPRS) on biomimetic systems to Christoph Wettstein, NUI Galway (Hardiman Research Scholarship to Ciara Kyne, Millennium Fund to PBC), Science Foundation Ireland (grant 10/RFP/BIC2807 to Peter B. Crowley) and the European Cooperation in Science and Technology (COST Action TD1003 – Bioinspired Nanotechnologies).

Table 1. Chemical shift perturbation (Δδ) observed for cyt *c* in the presence of different DNA concentrations at pH 7.0 and pH 6.0*

	pH 7.0, 30 mM NaCl								pH 6.0, 30 mM NaCl	
[DNA] μM	3.0		6.0		18.0		24.0		6.0	
Residue	$\Delta\delta\ ^{1}H$	$\Delta\delta\ ^{15}N$	$\Delta\delta\ ^{1}H$	$\Delta\delta\ ^{15}N$	$\Delta\delta\ ^{1}H$	$\Delta\delta\ ^{15}N$	$\Delta\delta\ ^{1}H$	$\Delta\delta\ ^{15}N$	$\Delta\delta\ ^{1}H$	$\Delta\delta\ ^{15}N$
K5	0.01	0.00	0.00	0.00	0.00	0.00	0.01	0.00	0.02	0.68
G6	0.01	0.10	0.01	0.15	0.01	0.31	0.02	0.31	0.00	0.14
K7	0.03	0.02	0.04	0.15	0.06	0.23	0.07	0.31	0.02	0.15
K8	0.00	0.00	0.01	0.25	0.01	0.41	0.00	0.41	0.01	0.30
I9	0.01	0.01	0.03	0.01	0.03	0.02	0.04	0.01	0.04	0.00
Q12	0.01	0.01	0.02	0.03	0.03	0.28	0.03	0.18	0.03	0.14
Q16	0.03	0.14	0.04	0.14	0.09	0.30	0.09	0.29	0.05	0.02
C17	0.01	0.01	0.00	0.01	0.01	0.01	0.01	0.01	0.02	0.15
H18	0.02	0.16	0.00	0.16	0.02	0.17	0.04	0.03	0.03	0.13
T19	0.01	0.00	0.00	0.00	0.02	0.16	0.02	0.00	0.01	0.04
V20	0.00	0.01	0.03	0.01	0.03	0.01	0.03	0.13	0.04	0.01
L32	0.00	0.01	0.05	0.10	0.00	0.00	0.04	0.31	0.04	0.01
L35	0.00	0.00	0.01	0.02	0.03	0.14	0.01	0.02	0.00	0.02
G37	0.00	0.01	0.00	0.01	0.00	0.00	0.01	0.09	0.06	0.17
G45	bbd	bbd	bbd	bbd	0.02	0.31	0.02	0.31	0.00	0.13
T47	bbd	bbd	bbd	bbd	bbd	bbd	bbd	bbd	0.02	0.00
N54	0.01	0.07	0.02	0.15	0.03	0.17	0.03	0.17	0.02	0.12
E61	0.01	0.14	0.03	0.10	0.07	0.06	bbd	bbd	0.04	0.01
E62	0.01	0.15	0.02	0.02	0.04	0.08	0.04	0.15	0.02	0.00
L68	0.00	0.01	0.00	0.00	0.01	0.18	0.01	0.00	0.02	0.12
G69	0.01	0.08	0.01	0.15	0.02	0.16	0.02	0.15	0.00	0.16
N70	0.00	0.08	0.00	0.06	0.01	0.22	0.01	0.08	0.07	0.00
K72	0.03	0.02	0.05	0.16	0.09	0.17	0.09	0.17	0.06	0.02
K73	0.02	0.00	0.03	0.00	0.04	0.01	0.04	0.16	0.04	0.02
Y74	0.01	0.00	0.02	0.06	0.04	0.15	0.04	0.16	0.03	0.02
I75	0.00	0.15	0.01	0.13	0.02	0.15	0.08	0.15	0.02	0.14
I85	0.05	0.01	0.04	0.01	0.04	0.00	0.04	0.01	0.03	0.01
K86	0.06	0.46	0.08	0.45	0.09	0.20	0.09	0.30	0.04	0.00
K87	0.03	0.07	0.04	0.08	0.07	0.06	0.07	0.07	0.05	0.00
K88	0.00	0.00	0.00	0.00	0.00	0.00	0.00	0.00	0.06	0.00
T89	0.03	0.01	0.05	0.15	0.08	0.24	0.09	0.32	0.08	0.29
E90	0.01	0.00	0.03	0.44	0.04	0.16	0.05	0.16	0.03	0.17
R91	0.02	0.00	0.00	0.44	0.04	0.00	0.05	0.00	0.04	0.14
E92	0.00	0.00	0.01	0.01	0.02	0.00	0.01	0.01	0.06	0.00
K100	0.00	0.08	0.01	0.15	0.01	0.15	0.02	0.15	0.02	0.01
A101	0.00	0.00	0.01	0.00	0.02	0.05	0.02	0.00	0.02	0.15
Σ of residues with sign. csps	12		22		29		26		26	

*A significant Δδ was defined as $^{1}H \geq 0.03$ or $^{15}N \geq 0.15$ ppm. bbd = broadened beyond detection.

Figure 1

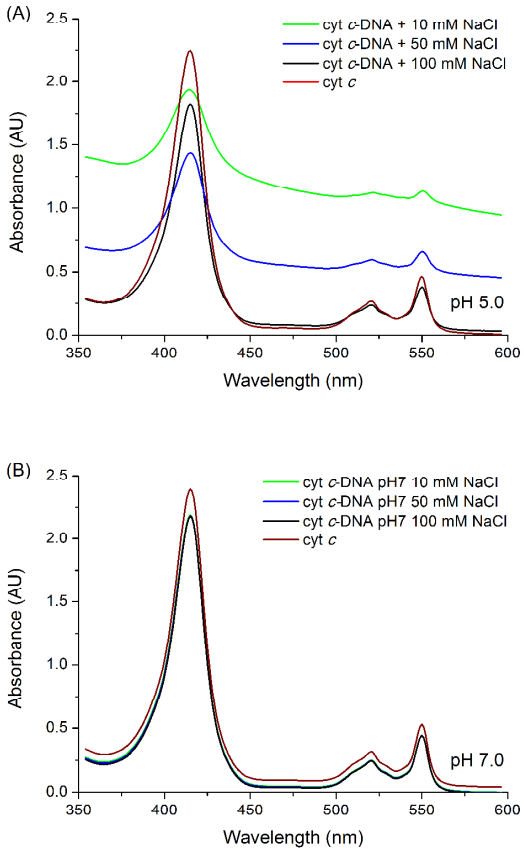

Figure 1. UV-vis absorption spectra of cyt *c*-DNA mixtures at pH (A) 5.0 and (B) 7.0 with increasing salt concentrations at RT. Samples of the complex contained 18 µM cyt *c* (red) and 3 µM DNA (ratio 0.17) in 20 mM KPi, 0.1 mM ascorbic acid and 10 mM NaCl (green) 50 mM NaCl (blue) and 100 mM NaCl (light grey).

Figure 2

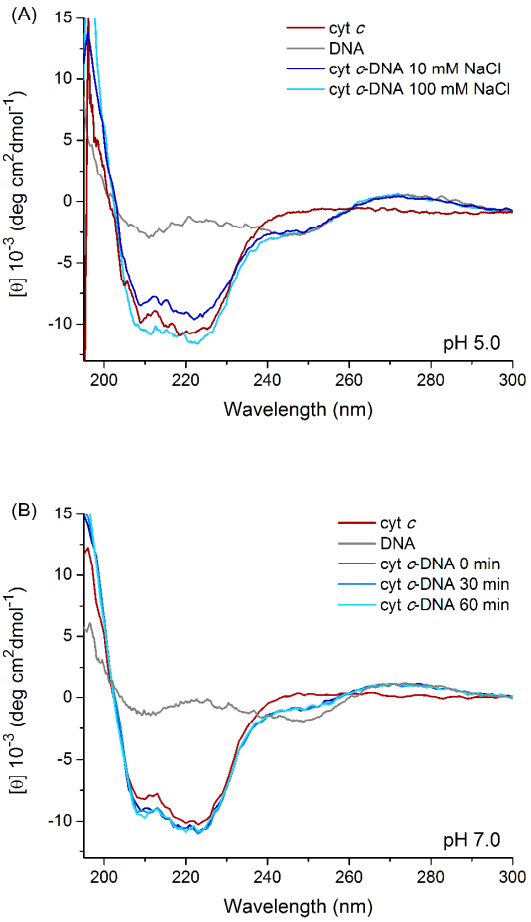

Figure 2. CD spectra of cyt *c* in the presence of DNA at (A) pH 5.0 and (B) pH 7.0. The samples contained 10 µM cyt *c* and 1.2 µM DNA (ratio 0.12) in 20 mM KPi with 10 mM NaCl and were measured after 60 min of incubation. (A) Cyt *c*-DNA at pH 5.0. The α-helical signal at 222 nm and 208 nm decreases in presence of DNA (dark blue) while the DNA signal (grey) at 280 nm stays constant. Increasing the salt concentration to 100 mM NaCl (light blue) resets the cyt *c* double peaks. The presence of Cl^- disturbs the CD signal below 190 nm. (B) Cyt *c*-DNA at pH 7.0 and with 10 mM NaCl, with no change in negative ellipticity after 0, 30 and 60 min of incubation.

Figure 3

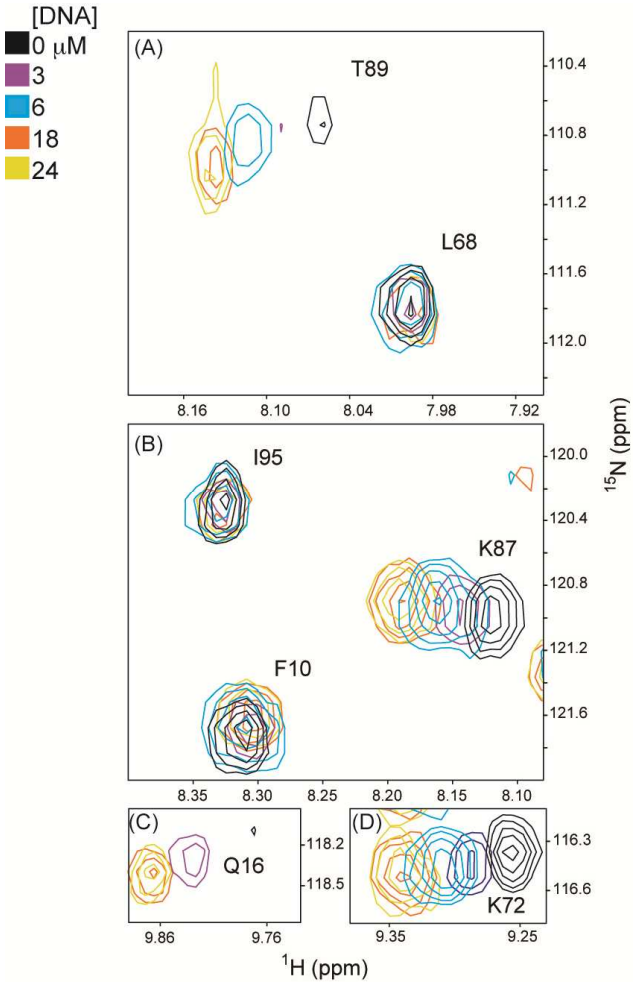

Figure 3. Various spectral regions (panels A-D) from overlaid ^{1}H-^{15}N TROSY-HSQC (600 MHz) of 50 μM pure cyt *c* (black contours) and cyt *c* plus DNA: 3.0 μM (purple), 6.0 μM (blue), 18.0 μM (orange) and 24.0 μM (yellow) (ratio from 0.06 to 0.48). The buffer was 20 mM KPi, 30 mM NaCl, pH 7.0.

Figure 4

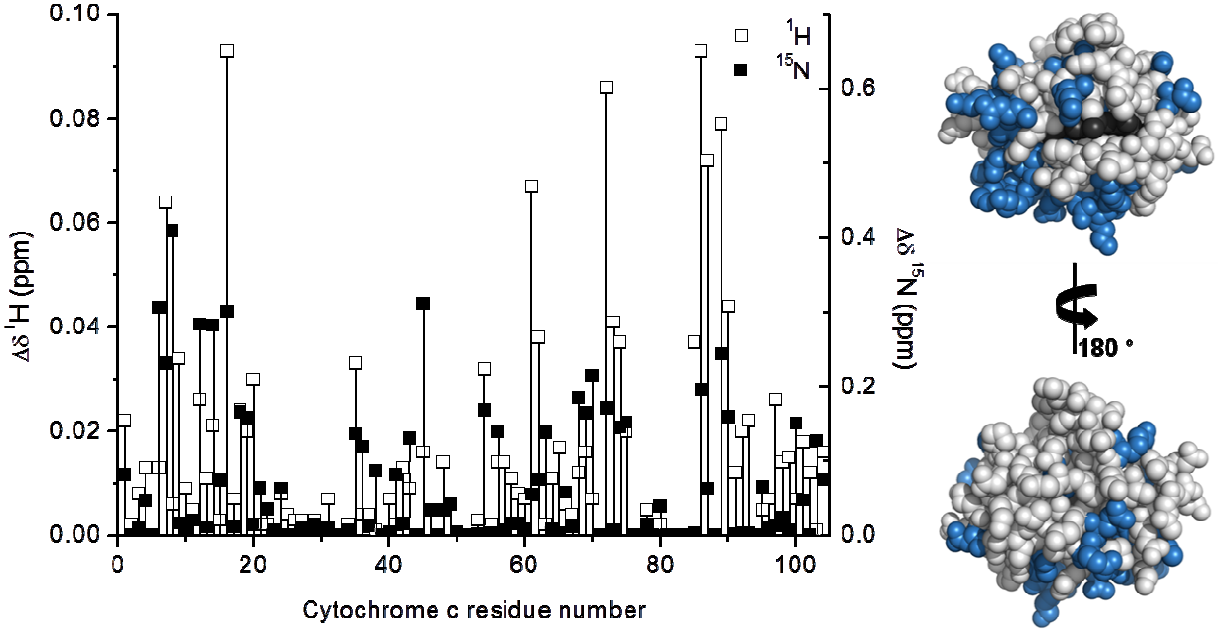

Figure 4. Plot of chemical shift perturbations (Δδ) for cyt *c* backbone amides in the presence of 18 μM DNA. The residues are numbered from 1 to 104. Blanks correspond to prolines (residues 30, 44, 71 and 76), unassigned residues (G84 and T47) and resonances that were broadened beyond detection. Right panel: Space filling representation of cyt *c* showing residues with a significant Δδ ($^{1}H \geq 0.03$ or $^{15}N \geq 0.15$ ppm) coloured blue. The heme is dark grey.

Figure 5

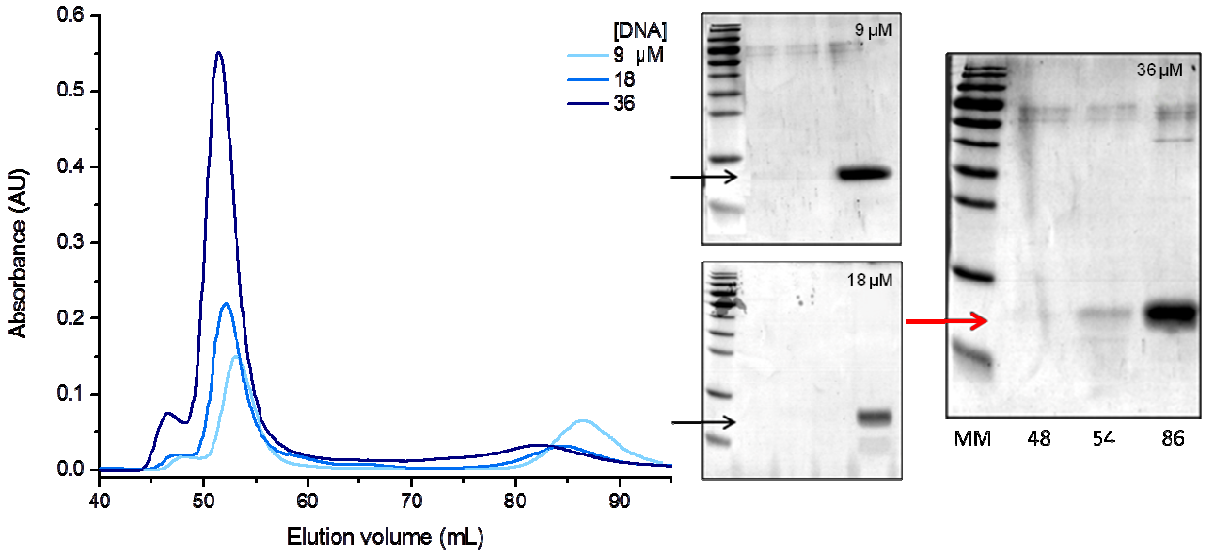

Figure 5. Left: Overlaid chromatograms from SEC experiments performed at pH 7.0. Samples contained 100 µM cyt *c* mixed with DNA at concentrations of: 9 µM (light blue), 18 µM (blue) and 36 µM (dark blue) (ratio from 0.09 to 0.36). Right: 15 % SDS-PAGE analysis of SEC fractions at 45, 54 and 80 mL, panel labelled according to DNA concentration ratio. The gel lanes are labelled: MM: molecular weight marker; fraction volume 45, 54 and 80 (mL). The black arrows mark the migration position of cyt *c*, the red arrow marks the co-eluted cyt *c* at high DNA concentration.

REFERENCES

1 Kalodimos, C.; Biris, N.; Bonvin, A.; Levandoski, M.; Guennuegues, M.; Boelens, R.; Kaptein, R. *Science* 2004, *305*, 386.
2 Pingoud, A.; Fuxreiter, M.; Pingoud, V.; Wende, W. *Cell. Mol. Life Sci.* 2005, *62*, 685.
3 Deibert, M.; Grazulis, S.; Sasnauskas, G.; Siksnys, V.; Huber, R. *Nat. Struct. Biol.* 2000, *7*, 792.
4 Littlefield, O.; Nelson, H. *Proteins: Struct., Funct., Genet.* 2001, *45*, 219.
5 Halford, S. E.; Marko, J. F. *Nucleic Acids Res.* 2004, *32*, 3040.
6 Bock, L. C.; Griffin, L. C.; Latham, J. A.; Vermaas, E. H.; Toole, J. J. *Nature* 1992, *355*, 564.
7 Lisdat, F.; Utepbergenov, D.; Haseloff, R. F.; Blasig, I. E.; Stocklein, W.; Scheller, F. W.; Brigelius-Flohe, R. *Anal. Chem.* 2001, *73*, 957.
8 Tolstonog, G.; Li, G.; Shoeman, R.; Traub, P. *DNA Cell Biol.* 2005, *24*, 85.
9 Viadiu, H.; Aggarwal, A. K. *Mol. Cell* 2000, *5*, 889.
10 Khrapunov, S.; Dragan, A.; Sivolob, A.; Zagariya, A. *Biochim. Biophys. Acta, Gene Struct. Expression* 1997, *1351*, 213.
11 Berg, J. M.; Tymoczko, J. L.; Stryer, L. *Biochemistry*, 7th ed.; W.H. Freeman: New York, 2012.
12 McGovern, R. E.; Fernandes, H.; Khan, A. R.; Power, N. P.; Crowley, P. B. *Nat. Chem.* 2012, *4*, 527.
13 Kuzuya, A.; Komiyama, M. *Nanoscale* 2010, *2*, 310.
14 Flory, J. D.; Simmons, C. R.; Lin, S.; Johnson, T.; Andreoni, A.; Zook, J.; Ghirlanda, G.; Liu, Y.; Yan, H.; Fromme, P. *J. Am. Chem. Soc.* 2014, *136*, 8283.
15 Andersen, F. F.; Knudsen, B.; Oliveira, C. L. P.; Frohlich, R. F.; Kruger, D.; Bungert, J.; Agbandje-McKenna, M.; McKenna, R.; Juul, S.; Veigaard, C.; Koch, J.; Rubinstein, J. L.; Guldbrandtsen, B.; Hede, M. S.; Karlsson, G.; Andersen, A. H.; Pedersen, J. S.; Knudsen, B. R. *Nucleic Acids Res.* 2008, *36*, 1113.
16 Erben, C. M.; Goodman, R. P.; Turberfield, A. J. *Angew. Chem., Int. Ed.* 2006, *45*, 7414.
17 Sarauli, D.; Tanne, J.; Schaefer, D.; Schubart, I. W.; Lisdat, F. *Electrochem. Commun.* 2009, *11*, 2288.
18 Scott, R. A.; Mauk, A. G. *Cytochrome C: a multidisciplinary approach*; University Science Books: Sausalito, Calif., 1996.
19 Feng, Z. Q.; Imabayashi, S.; Kakiuchi, T.; Niki, K. *J. Chem. Soc., Faraday Trans.* 1997, *93*, 1367.
20 Katz, E.; Zayats, M.; Willner, I.; Lisdat, F. *Chem. Commun.* 2006, 1395.
21 Lisdat, F.; Dronov, R.; Moehwald, H.; Scheller, F. W.; Kurth, D. G. *Chem. Commun.* 2009, 274.
22 Wegerich, F.; Turano, P.; Allegrozzi, M.; Mohwald, H.; Lisdat, F. *Anal. Chem.* 2009, *81*, 2976.
23 Scheller, W.; Jin, W.; Ehrentreich-Forster, E.; Ge, B.; Lisdat, F.; Buttemeier, R.; Wollenberger, U.; Scheller, F. W. *Electroanalysis* 1999, *11*, 703.
24 Cooper, J. M.; Greenough, K. R.; McNeil, C. J. *J. Electroanal. Chem.* 1993, *347*, 267.
25 Gobi, K. V.; Mizutani, F. *J. Electroanal. Chem.* 2000, *484*, 172.
26 Bushnell, G. W.; Louie, G. V.; Brayer, G. D. *J. Mol. Biol.* 1990, *214*, 585.
27 Bashir, Q.; Volkov, A. N.; Ullmann, G. M.; Ubbink, M. *J. Am. Chem. Soc.* 2010, *132*, 241.

28 Crowley, P. B.; Carrondo, M. A. *Proteins: Struct., Funct., Bioinf.* 2004, *55*, 603.
29 Crowley, P. B.; Chow, E.; Papkovskaia, T. *Chembiochem* 2011, *12*, 1043.
30 Collinson, M.; Bowden, E. F.; Tarlov, M. J. *Langmuir* 1992, *8*, 1247.
31 Song, S.; Clark, R. A.; Bowden, E. F.; Tarlov, M. J. *J. Phys. Chem.* 1993, *97*, 6564.
32 Ikeda, O.; Shirota, Y.; Sakurai, T. *J. Electroanal. Chem.* 1990, *287*, 179.
33 Lisdat, F.; Ge, B.; Scheller, F. W. *Electrochem. Commun.* 1999, *1*, 65.
34 Lao, R.; Wang, L.; Wan, Y.; Zhang, J.; Song, S.; Zhang, Z.; Fan, C.; He, L. *Int. J. Mol. Sci.* 2007, *8*, 1.
35 Shao, Y.; Morita, K.; Dai, Q.; Nishizawa, S.; Teramae, N. *Electrochem. Commun.* 2008, *10*, 438.
36 Wettstein, C.; Moehwald, H.; Lisdat, F. *Bioelectrochemistry* 2012, *88*, 97.
37 Beissenhirtz, M. K.; Scheller, F. W.; Lisdat, F. *Anal. Chem.* 2004, *76*, 4665.
38 Bonk, S.; Lisdat, F. *Biosens. Bioelectron.* 2009, *25*, 739.
39 Feifel, S. C.; Lisdat, F. *J. Nanobiotechnol.* 2011, *9*.
40 Feifel, S. C.; Kapp, A.; Ludwig, R.; Gorton, L.; Lisdat, F. *RSC Adv.* 2013, *3*, 3428.
41 Patel, C. N.; Lind, M. C.; Pielak, G. J. *Protein Expression and Purification* 2001, *22*, 220.
42 Volkov, A. N.; Vanwetswinkel, S.; Van de Water, K.; van Nuland, N. A. J. *J. Biomol. NMR* 2012, *52*, 245.
43 Worrall, J. A. R.; Kolczak, U.; Canters, G. W.; Ubbink, M. *Biochemistry* 2001, *40*, 7069.
44 van Gelder, B.; Slater, E. C. *Biochim. Biophys. Acta* 1962, *58*, 593.
45 Liu, W. X.; Rumbley, J.; Englander, S. W.; Wand, A. J. Protein Sci. 2003, *12*, 2104.
46 Cai, X. M.; Dass, C. *Curr. Org. Chem.* 2003, *7*, 1841.
47 Dickerson, R. E.; Kopka, M. L.; Weinzierl, J.; Varnum, J.; Eisenberg, D.; Margoliash, E. *J. Biol. Chem.* 1967, *242*, 3015.
48 Fisher, W. R.; Taniuchi, H.; Anfinsen, C. B. *J. Biol. Chem.* 1973, *248*, 3188.
49 Crowley, P. B.; Ubbink, M. *Acc. Chem. Res.* 2003, *36*, 723.
50 Volkov, A. N.; Worrall, J. A. R.; Holtzmann, E.; Ubbink, M. *Proc. Natl. Acad. Sci. U. S. A.* 2006, *103*, 18945.
51 Volkov, A. N.; Bashir, O.; Worrall, J. A. R.; Ubbink, M. *J. Mol. Biol.* 2009, *385*, 1003.
52 Pelletier, H.; Kraut, J. *Science* 1992, *258*, 1748.